JOURNAL OF BACTERIOLOGY, Mar. 2001, p. 2013–2024 Vol. 183, No. 6
0021-9193/01/$04.00+0 DOI: 10.1128/JB.183.6.2013–2024.2001
Copyright © 2001, American Society for Microbiology. All Rights Reserved.

Mobile Cytochrome c_2 and Membrane-Anchored Cytochrome c_y Are Both Efficient Electron Donors to the cbb_3- and aa_3-Type Cytochrome *c* Oxidases during Respiratory Growth of *Rhodobacter sphaeroides*

FEVZI DALDAL,[1]* SEVNUR MANDACI,[1,2] CHRISTINE WINTERSTEIN,[1] HANNU MYLLYKALLIO,[1]† KRISTEN DUYCK,[1] AND DAVIDE ZANNONI[3]

Department of Biology, Plant Science Institute, University of Pennsylvania, Philadelphia, Pennsylvania 19104[1]; Marmara Research Center, Research Institute for Genetic Engineering and Biotechnology, Gebze, Kocaeli 41470, Turkey[2]; and Department of Biology, University of Bologna, Bologna 40126, Italy[3]

Received 25 September 2000/Accepted 31 October 2000

We have recently established that the facultative phototrophic bacterium *Rhodobacter sphaeroides*, like the closely related *Rhodobacter capsulatus* species, contains both the previously characterized mobile electron carrier cytochrome c_2 (cyt c_2) and the more recently discovered membrane-anchored cyt c_y. However, *R. sphaeroides* cyt c_y, unlike that of *R. capsulatus*, is unable to function as an efficient electron carrier between the photochemical reaction center and the cyt bc_1 complex during photosynthetic growth. Nonetheless, *R. sphaeroides* cyt c_y can act at least in *R. capsulatus* as an electron carrier between the cyt bc_1 complex and the cbb_3-type cyt *c* oxidase (cbb_3-C_{ox}) to support respiratory growth. Since *R. sphaeroides* harbors both a cbb_3-C_{ox} and an aa_3-type cyt *c* oxidase (aa_3-C_{ox}), we examined whether *R. sphaeroides* cyt c_y can act as an electron carrier to either or both of these respiratory terminal oxidases. *R. sphaeroides* mutants which lacked either cyt c_2 or cyt c_y and either the aa_3-C_{ox} or the cbb_3-C_{ox} were obtained. These double mutants contained linear respiratory electron transport pathways between the cyt bc_1 complex and the cyt *c* oxidases. They were characterized with respect to growth phenotypes, contents of *a*-, *b*-, and *c*-type cytochromes, cyt *c* oxidase activities, and kinetics of electron transfer mediated by cyt c_2 or cyt c_y. The findings demonstrated that both cyt c_2 and cyt c_y are able to carry electrons efficiently from the cyt bc_1 complex to either the cbb_3-C_{ox} or the aa_3-C_{ox}. Thus, no dedicated electron carrier for either of the cyt *c* oxidases is present in *R. sphaeroides*. However, under semiaerobic growth conditions, a larger portion of the electron flow out of the cyt bc_1 complex appears to be mediated via the cyt c_2-to-cbb_3-C_{ox} and cyt c_y-to-cbb_3-C_{ox} subbranches. The presence of multiple electron carriers and cyt *c* oxidases with different properties that can operate concurrently reveals that the respiratory electron transport pathways of *R. sphaeroides* are more complex than those of *R. capsulatus*.

The purple nonsulfur facultative phototrophic bacteria of *Rhodobacter* species, *Rhodobacter capsulatus* and its close relative *Rhodobacter sphaeroides*, are excellent model organisms for studying cellular energy transduction (46). They have versatile growth modes and are capable of both anoxygenic phototrophic (Ps) and vigorous respiratory (Res) growth in the presence of oxygen. They contain a photochemical reaction center (RC) (43, 44), a ubihydroquinone:cytochrome *c* (cyt *c*) oxidoreductase (cyt bc_1 complex) (6, 45), and a *c*-type cytochrome as a mobile electron carrier (7, 8), but their Ps and Res electron transport chains are different (46, 47).

During the Ps growth of *R. capsulatus*, electrons are conveyed from the cyt bc_1 complex to the RC either by the well-studied mobile electron carrier cyt c_2 (7) or the more recently discovered membrane-anchored electron carrier cyt c_y (17), encoded by *cycA* and *cycY*, respectively. On the other hand, in *R. sphaeroides*, the Ps electron transport pathway can be mediated only by a mobile electron carrier like cyt c_2 (8) or its functional analogues such as isocyt c_2 (33) (Fig. 1). Although Ps-grown cells of *R. sphaeroides* also harbor a membrane-anchored cyt c_y, this electron carrier is not able to support Ps growth (27). Yet the Ps growth inability of *R. sphaeroides* mutants lacking cyt c_2 can be restored readily by genetic introduction of *R. capsulatus* cyt c_y (17, 18). These findings indicate that *R. sphaeroides* cyt c_y is the culprit for the Ps growth inability of this species in the absence of cyt c_2 (27), but the molecular basis of this observation remains unknown.

Respiratory electron transport pathways of *R. capsulatus* and *R. sphaeroides* are also similar but not identical (46) (Fig. 1). Both species contain a respiratory electron transport pathway that is branched after the quinone pool. One of these branches contains hydroquinone oxidases (Q_{ox}) commonly found in microbes, while the other one harbors a mitochondrial-like cyt *c* oxidase(s) (C_{ox}) converting oxygen to water (13). While *R. capsulatus* contains only one cbb_3-type C_{ox} (cbb_3-C_{ox}) (14, 19), both an aa_3-type C_{ox} (aa_3-C_{ox}) (16, 36), and a cbb_3-C_{ox} (12, 42) are present in *R. sphaeroides*. In the latter species, the cbb_3-C_{ox} is predominant in microaerobic or Ps-grown cells, while the aa_3-C_{ox} becomes a major component under high O_2 tension (37). In both species, the nature of the Q_{ox} is not well known. Recent works including genome sequences (4, 11) suggest the

* Corresponding author. Mailing address: Department of Biology, Plant Science Institute, University of Pennsylvania, Philadelphia, PA 19104. Phone: (215) 898-4394. Fax: (215) 989-8780. E-mail: fdaldal@sas.upenn.edu.

† Present address: Institut de Génétique et Microbiologie, Université Paris XI, 91405 Orsay Cedex, France.

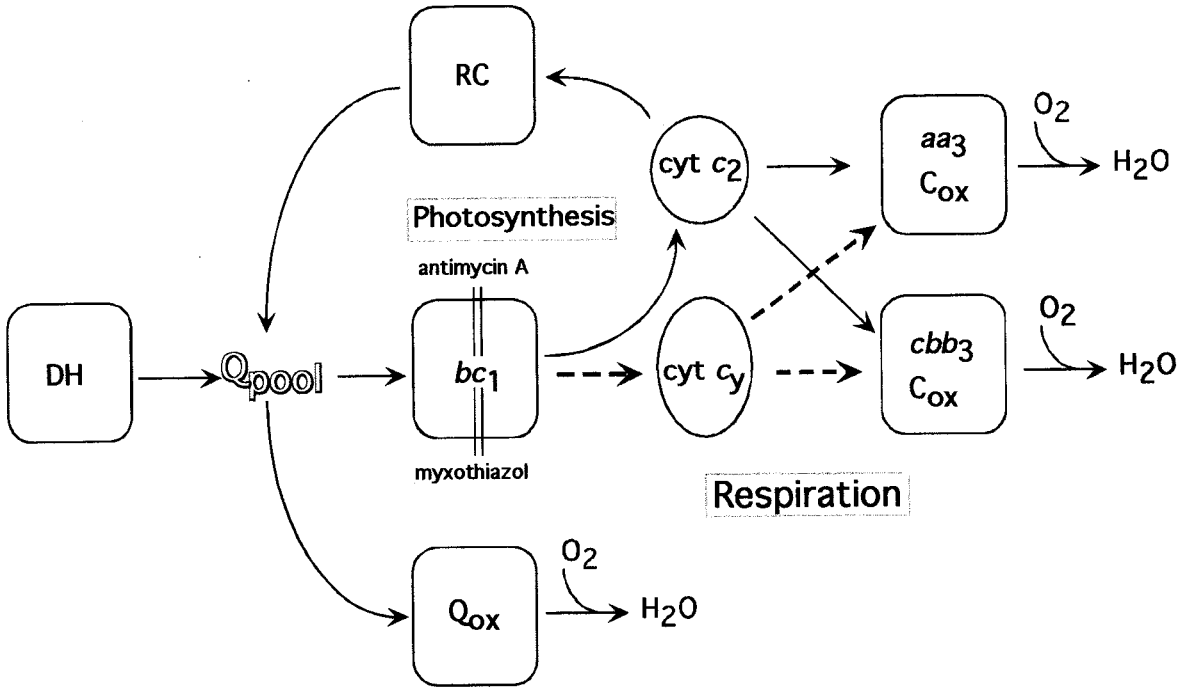

FIG. 1. Photosynthetic and respiratory electron transport pathways of *R. sphaeroides.* DH, Q_{pool}, bc_1, RC, Q_{ox}, cyt c_2, cyt c_y, aa_3-C_{ox}, and cbb_3-C_{ox} correspond to the respiratory NADH and succinate dehydrogenases, membrane quinone pool, cyt bc_1 complex, photochemical reaction center, hydroquinone oxidase, soluble electron carrier cyt c_2, membrane-attached electron carrier cyt c_y, aa_3-type cyt *c* oxidase, and cbb_3-type cyt *c* oxidase, respectively. Dotted arrows highlight the electron transfer pathways catalyzed by cyt c_y. Antimycin A (Ant A) and myxothiazol (Myx) are inhibitors of the cyt bc_1 complex.

presence of one Q_{ox} in *R. capsulatus* (21, 48; K. Zhang and F. Daldal, unpublished data) and possibly two Q_{ox} in *R. sphaeroides*.

Recently, we have established that *R. sphaeroides* cyt c_y can function as an electron carrier between the cyt bc_1 complex and the cbb_3-C_{ox} in *R. capsulatus* (27). This finding raised the issue of whether it can also act as an electron carrier during the Res growth of *R. sphaeroides* and, if so, whether it can donate electrons to both the aa_3-C_{ox} and the cbb_3-C_{ox}. Obviously, the presence of two *c*-type electron carriers and two cyt *c* oxidases complicates this analysis. To facilitate it, appropriate mutations inactivating either cyt c_2 or cyt c_y were introduced into *R. sphaeroides* strains lacking either cbb_3-C_{ox} or aa_3-C_{ox} activity. The double mutants thus obtained converted the crisscrossed respiratory electron transport pathways into simpler linear pathways (Fig. 1) and allowed estimation of their efficiencies. The data demonstrated for the first time that in *R. sphaeroides* either cyt c_2 or cyt c_y can act as an electron carrier between the cyt bc_1 complex and either the cbb_3-C_{ox} or the aa_3-C_{ox}. Furthermore, they indicated that electron flow via the cyt $c_2 \rightarrow cbb_3$-C_{ox} and cyt $c_y \rightarrow cbb_3$-C_{ox} subbranches appears to be greater under semiaerobic growth conditions. During these studies, it was noted that in the absence of the latter respiratory pathway, light-harvesting protein complexes, which are usually absent in the presence of oxygen, were also produced.

MATERIALS AND METHODS

Bacterial strains and growth conditions. *Escherichia coli* strains were grown on Luria broth (LB medium) supplemented with kanamycin, spectinomycin, or tetracycline at a final concentration of 50, 50, or 12.5 μg per ml, respectively. *R. sphaeroides* strains were grown in Sistrom's minimal medium (Med A) (40) supplemented as needed with 10, 10, or 2.5 μg of spectinomycin, kanamycin, or tetracycline, respectively, per ml. For semiaerobic growth, 2-liter flasks were filled with 1 liter of growth medium and shaken at 150 rpm with a rotary shaker (New Brunswick Scientific Co. Inc., Rutherford, N.J.). Photo- or chemoheterotrophic growth phenotypes and ability to catalyze the Nadi reaction (*N',N'*-dimethyl-*p*-phenylenediamine + α-naphthol → indophenol blue + H_2O) (24) were determined on solid media using cells grown in anaerobic jars containing H_2- and CO_2-generating gas packs (BBL) or an aerobic dark incubator at 35°C in the presence of atmospheric oxygen. Growth rates of various strains were determined using liquid cultures inoculated with freshly grown cells at appropriate dilutions. As needed, cultures were first incubated overnight at ambient temperature without shaking and then transferred to a rotary shaker at 35°C, and the turbidity was monitored using side-arm flasks and a Klett-Summerson colorimeter. All strains and plasmids used are listed in Table 1. The parental *R. sphaeroides* strain Ga (40) is referred to as wild type with respect to its cytochrome profile and its Ps and Res growth properties.

Molecular genetic techniques and construction of various *R. sphaeroides* mutants. Two different insertion-deletion alleles of *cycA* and *cycY*, carrying either spectinomycin resistance (Spe^r) or kanamycin resistance (Kan^r)-conferring gene cartridges, were necessary for constructing various double mutants lacking cyt c_2 or cyt c_y and cbb_3-C_{ox} or aa_3-C_{ox}. Thus, a *cycY*::*kan* allele was constructed similarly to *cycY*::*spe* described previously (27), except that a Kan^r-conferring cartridge instead of a Spe^r-conferring cartridge from pHP45Ω-K (9) was used. The desired allele was transferred into the suicide plasmid pSup202, conferring tetracycline resistance (Tet^r), and via the *E. coli* donor strain S17.1 (39) conjugated into the appropriate *R. sphaeroides* strains, selecting for Spe^r or Kan^r as required. Among the transconjugants, those that were Tet^s, and hence carrying a chromosomal allele replacement via a double-crossover event, were retained for further analyses (3). Introduction of appropriate *cycA* and *cycY* alleles into the *R. sphaeroides* Δ(*ccoNO*::*kan*) (MT001) and Δ(*ctaD*::*spe*) (JS100) mutants yielded the Δ(*cycA*::*spe*) Δ(*ccoNO*::*kan*) (KD02) and Δ(*cycY*::*spe*) Δ(*ccoNO*::*kan*) (KD04) and the Δ(*cycY*::*kan*) Δ(*ctaD*::*spe*) (KD03) and Δ(*cycA*::*kan*) Δ(*ctaD*::*spe*) (KD05) double mutants, respectively (Table 1).

Biochemical and spectroscopic techniques. *R. sphaeroides* chromatophore membranes from washed cells grown semiaerobically in Med A were prepared

TABLE 1. Bacterial strains and plasmids used in this work

Strain or plasmid	Genotype	Relevant phenotype	Source or reference
E. coli			
HB101	F *proA2 hsdS20 recA1 ara-14 lacY1 galK2 rpsL20 supE44 xyl-5 mtl-1*	r_B^- m_B^-	Stratagene
S17.1	*thi pro hsdR recA ara* RP4::2-Tc::Mu::*kan*:Tn*7* integrated into chromosome	r_B^- m_B^+ Tp^r Sm^r	39
R. sphaeroides			
Ga	crt	Wild type	40
Gadc2	*crt* Δ(*cycA*::*spe*)	Cyt c_2^-	3
Gadcy	*crt* Δ(*cycY*::*kan*)	Cyt c_y^-	17
Gadc2cy	*crt*, Δ(*cycA*::*spe*) Δ(*cycY*::*kan*)	Cyt c_2^- Cyt c_y^-	17
MT001	*crt* Δ(*ccoNO*::*kan*)	cbb_3-C_{ox}^-	42
KD02	*crt* Δ(*cycA*::*spe*) Δ(*ccoNO*::*kan*)	Cyt c_2^- cbb_3-C_{ox}^-	This work
KD04	*crt* Δ(*cycY*::*spe*) Δ(*ccoNO*::*kan*)	Cyt c_y^- cbb_3-C_{ox}^-	This work
JS100	*crt* Δ(*ctaD*::*spe*)	aa_3-C_{ox}^-	36
KD03	*crt* Δ(*cycY*::*kan*) Δ(*ctaD*::*spe*)	Cyt c_y^- aa_3-C_{ox}^-	This work
KD05	*crt* Δ(*cycA*::*kan*) Δ(*ctaD*::*spe*)	Cyt c_2^- aa_3-C_{ox}^-	This work
ME127	*crt* Δ(*ctaD*::*spe*) Δ(*ccoNO*::*kan*)	cbb_3-C_{ox}^- aa_3-C_{ox}^-	42
BC17	*crt* Δ(*petABC*(*fbcFBC*)::*kan*)	Cyt bc_1^-	45
Plasmids			
pBSII	pBlueScript II KS(+)	Amp^r	Stratagene
pHP45Ω	*spe* cartridge	Spe^r	31
pHP45Ω-Km	*kan* cartridge	Kan^r	9
pSup202	Suicide plasmid	Tet^r Cm^r Amp^r	39
p4.2	*cycY*::*kan* in *Pst*I site of pSup202		This work
pcycA::spe	*cycA*::*spe* in *Pst*I site of pSup202		This work
pKD10.2	2-kb *spe* cartridge of pHP45Ω in *Bam*HI site of *cyc*Y carried by pU2000 (in opposite orientation of *cyc*Y)		This work
pU2000	1.8-kb *Bgl*II-*Xba*I *R. sphaeroides* chromosomal DNA carrying *cycY* in pBSII KS(+)		51
pKD11	3 kb *cycY*::*spe* fragment in *Eco*RI site of pSup202		This work
pSupC2 P2.71::kan	Δ(*cycA*::*kan*) at *Stu*I site of *cyc*A carried at *Pst*I site of pSup202		8

using a French pressure cell at 18,000 lb/in^2 and ultracentrifugation either in 50 mM 3-(*N*-morpholino)propanesulfonic acid (MOPS) buffer (pH 7.0) containing 1 mM KCl, EDTA, and phenylmethylsulfonyl fluoride for polyacrylamide gel electrophoresis (PAGE) analyses (18, 20) or in 50 mM MOPS buffer (pH 7.2) containing 5 mM $MgCl_2$ for spectroscopic studies (50). Membrane fragments were washed twice, resuspended at a known protein concentration in the same buffer, and stored frozen at −80°C until further use. Protein content of the samples was determined by the method of Bradford (2) or Lowry et al. (22), using bovine serum albumin as a standard. Bacteriochlorophyll concentration was measured by the optical absorption of acetone-methanol (7:2, vol/vol) extracts, using an extinction coefficient ε_{775} of 75 mM^{-1} cm^{-1} (5). Sodium dodecyl sulfate (SDS)-PAGE was performed using 16.5% acrylamide Tris-Tricine gels as described by Schägger and von Jagow (35). Samples were denatured for 5 min at 37°C in SDS loading buffer prior to electrophoresis, and gels were stained with Coomassie brilliant blue to visualize the polypeptides. The *c*-type cytochromes were revealed via the intrinsic peroxidase activity of their heme group, using 3,3′,5,5′-tetramethylbenzidine (TMBZ) and H_2O_2 (41). The amounts of cytochromes in chromatophore membranes were estimated by recording at room temperature reduced (with ascorbate or dithionite)-minus-oxidized (with ferricyanide) optical difference spectra. Either a Hitachi 3400 or Jasco 7800 spectrophotometer and the extinction coefficients $\varepsilon_{604-630}$ of 23 mM^{-1} cm^{-1}, $\varepsilon_{561-575}$ of 22 mM^{-1} cm^{-1}, and $\varepsilon_{551-540}$ of 29 mM^{-1} cm^{-1} were used for *a*-, *b*-, and *c*-type cytochromes, respectively.

Cyt *c* oxidase activities in membrane fragments were determined using either reduced horse heart cyt *c* as a substrate or by monitoring O_2 consumption. In the first case, immediately prior to the assay, horse heart cyt *c* was reduced by addition of sodium dithionite, excess of which was eliminated via chromatography through a small column containing Sephadex G-10 as a matrix (14, 20). Oxidation of cyt *c* was monitored at 550 nm in a stirred cuvette, thermostated at 25°C, containing 50 mM Tris (pH 8.0) buffer supplemented with 0.1 mg of dodecyl maltoside per ml, 5 μM myxothiazol (Myx), and 40 μM reduced cyt *c*. As needed, 2 mM potassium cyanide (KCN) was used as an inhibitor (34). In the second case, respiratory rates were measured by polarography at 28°C with a Clark-type oxygen electrode (Yellow Springs Instruments Inc., Yellow Springs, Ohio). These assays used 0.25 to 0.30 mg of membrane fragments per ml resuspended in 50 mM MOPS buffer (pH 7.2) containing 5 mM $MgCl_2$, 2 mM sodium ascorbate, and 200 μM *N,N,N′,N′*-tetramethyl-*p*-phenylenediamine (TMPD) or 50 μM horse heart cyt *c* (15, 48). As needed, 100 μM KCN was used to determine the amount of C_{ox}-independent O_2 consumption during the assay, and enzymatic activities were expressed in moles of substrate consumed per minute per milligram of protein. TMPD was also substituted with 2,3,5,6-tetramethyl-1,4-phenylenediamine (DAD) or 3,6-dichlorophenol indophenol (DCIP) as an electron donor and KCN with NaN_3 as an inhibitor (34). Kinetic changes in the absorption of *c*-type cytochromes were monitored at 551 minus 540 nm at 28°C, using a Jasco V-550 dual-wavelength spectrophotometer equipped with a Jasco ETC-505T rapid-mixing and temperature control apparatus (15).

To estimate amounts of the light-harvesting complexes in membrane fragments of various *R. sphaeroides* mutants, 50-ml cultures were grown aerobically with vigorous shaking in 250-ml flasks to an optical density at 630 nm of less than 0.4. Cells were collected by centrifugation and resuspended in 50 mM potassium phosphate buffer (pH 7.0) containing 10 mM EDTA and leupeptin, pepstatin A, and Pefabloc SC (Roche Inc., Indianapolis, Ind.) as protease inhibitors at concentrations suggested by the supplier. After addition of 1/50 volume of lysozyme (10 mg/ml) and 1 h of incubation on ice, cells were frozen at −80°C for 10 min, thawed, and sonicated on ice for 5 min at a 40% relative output in a sonicator (model 150; Dynatech Laboratories Inc., Farmingdale, N.Y.). Cell debris was removed by centrifugation at 13,000 rpm for 30 min at 4°C, and the supernatants were centrifuged at 150,000 × *g* for 1 h. Membrane fragments thus obtained were washed with 50 mM potassium phosphate (pH 7.0) buffer containing 1 mM EDTA, resuspended in the same buffer, and stored at −80°C until further use. Optical absorption spectra were recorded between the wavelengths of 380 and 1,000 nm with a Beckman DU640 spectrophotometer, using an amount of *R. sphaeroides* membranes corresponding to a total protein content of 0.2 mg per ml in 10 mM potassium phosphate (pH 7.2) buffer containing 1 mM EDTA.

Chemicals. All chemicals, including the redox mediators, were of analytical grade and obtained from commercial sources as described previously (15). *n*-Dodecyl β-D-maltoside was from Anatrace; horse heart cyt *c* (type VI) and TMPD were from Sigma-Aldrich Chemical Co. (St. Louis, Mo.).

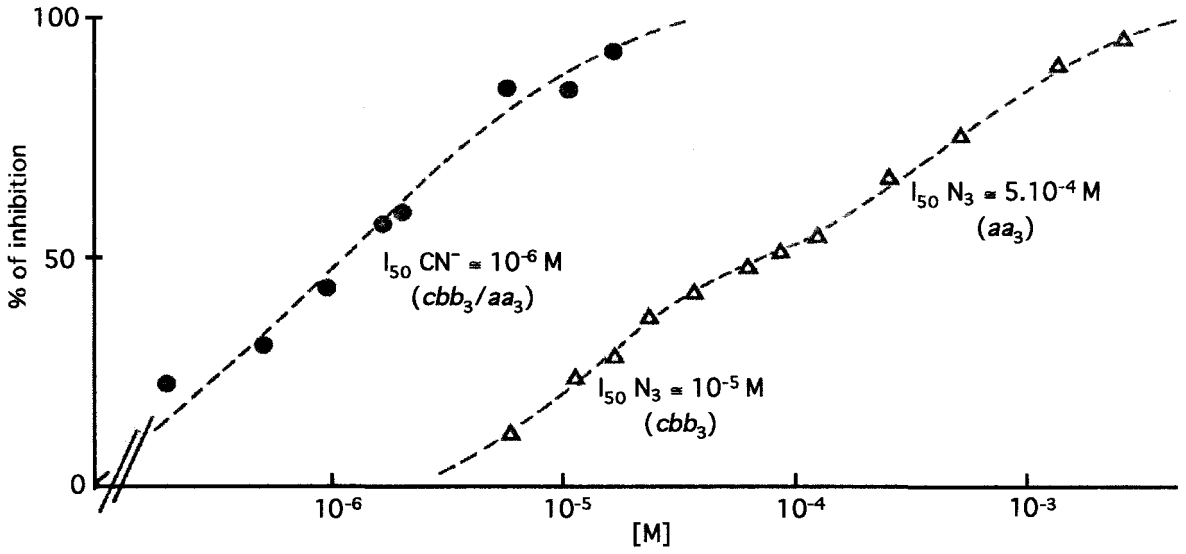

FIG. 2. Inhibition of the cyt *c* oxidase activity found in *R. sphaeroides* membranes. Inhibitory effects of CN^- (circles) and N_3^- (triangles) on ascorbate and cyt *c* oxidase activities found in membrane fragments of *R. sphaeroides* wild-type strain Ga were determined as described in Materials and Methods. aa_3 and cbb_3 correspond to the aa_3-C_{ox} and cbb_3-C_{ox}, respectively. See the text for details.

RESULTS

***R. sphaeroides* strain Ga cells grown under semiaerobic conditions contain both cbb_3-C_{ox} and aa_3-C_{ox} activities.** Both cbb_3-C_{ox} and aa_3-C_{ox} activities in the wild-type *R. sphaeroides* strain Ga can be fully inhibited by cyanide (CN^-) and azide (N_3^-) anions. However, while CN^- affects both C_{ox} activities similarly, N_3^- inhibits them differently (34). Thus, to assess whether cells grown under semiaerobic conditions contained both of these enzymes, ascorbate/cyt *c*-dependent C_{ox} activity was measured in the presence of increasing concentration of these inhibitors, using membranes of wild-type strain Ga (Fig. 2). The cbb_3-C_{ox} activity was totally inhibited by 100 μM N_3^-, whereas the aa_3-C_{ox} activity required 2 to 3 mM N_3^- for full inhibition. Moreover, the inhibition by CN^- was monophasic (90% inhibition at 20 μM KCN), while that by N_3^- was biphasic, with a decrease in slope around 100 μM NaN_3, corresponding to about 60% inhibition of total activity. Thus, the *R. sphaeroides* cells used in this study contained both of the C_{ox} activities simultaneously.

***R. sphaeroides* mutants with linear, *c*-type cytochrome-dependent respiratory electron transport pathways.** In *R. sphaeroides,* *c*-type cytochromes containing branches of the respiratory electron transport pathways are complicated due to the presence of the cyt c_2, cyt c_y, cbb_3-C_{ox}, and aa_3-C_{ox} (Fig. 1). To simplify these crisscrossed pathways, four double mutants containing only one electron carrier (cyt c_2 or cyt c_y) and one C_{ox} (cbb_3-C_{ox} or aa_3-C_{ox}) were obtained (Table 1). Growth phenotypes of these mutants confirmed that among the electron transport components mutated, only cyt c_2 was required for Ps growth (8) (Table 2). Their doubling times under Res growth conditions (about 100 to 120 min on Med A at 35°C) were similar to those of their parents, with the exception of the cbb_3-C_{ox}^- aa_3-C_{ox}^- double mutant (ME127), which grew slightly slower (doubling time of approximately 150 min). In particular,

TABLE 2. Electron transport chain components of various *R. sphaeroides* mutants, and their cytochrome contents in membranes[a]

Strain	Phenotype	Electron carrier(s)/cyt *c* oxidase(s)	Cyt *c* profile					Cyt *a*	Cyt *b*	Cyt *c*	Cyt *b*/Cyt *c* ratio
			c_p	c_1	c_o	c_y	c_2				
Ga	Ps^+ Res^+ $Nadi^+$	Cyt c_2 + cyt c_y/cbb_3-C_{ox} + aa_3-C_{ox}	+	+	+	+	+	0.8	2.2	3.8	0.57
Gadc2	Ps^- Res^+ $Nadi^+$	Cyt c_y/cbb_3-C_{ox} + aa_3-C_{ox}	+	+	+	+	−	0.34	1.0	1.3	0.77
Gadcy	Ps^+ Res^+ $Nadi^+$	Cyt c_2/cbb_3-C_{ox} + aa_3-C_{ox}	+	+	+	−	+	0.37	1.0	1.45	0.68
Gadc2cy	Ps^- Res^+ $Nadi^+$	None/cbb_3-C_{ox} + aa_3-C_{ox}	+	+	+	−	−	0.24	1.0	0.95	1.05
MT001	Ps^+ Res^+ $Nadi^{slow}$	Cyt c_2 + cyt c_y/aa_3-C_{ox}	−	+	−	+	+	0.48	1.15	1.14	1.0
KD02	Ps^- Res^+ $Nadi^{slow}$	Cyt c_y/aa_3-C_{ox}	−	+	−	+	−	0.42	0.93	0.7	1.3
KD04	Ps^+ Res^+ $Nadi^{slow}$	Cyt c_2/aa_3-C_{ox}	−	+	−	−	+	0.42	0.87	0.69	1.26
JS100	Ps^+ Res^+ $Nadi^+$	Cyt c_2 + cyt c_y/cbb_3-C_{ox}	+	+	+	+	+	ND[b]	1.2	1.9	0.63
KD03	Ps^+ Res^+ $Nadi^+$	Cyt c_y/cbb_3-C_{ox}	+	+	+	−	+	ND	1.42	1.65	0.86
KD05	Ps^- Res^+ $Nadi^+$	Cyt c_y/cbb_3-C_{ox}	+	+	+	+	−	ND	2.2	1.56	0.87
ME127	Ps^+ Res^+ $Nadi^-$	Cyt c_2 + cyt c_y/none	−	+	−	+	+	ND	1.28	1.06	1.2
BC17	Ps^- Res^+ $Nadi^+$	Cyt c_2 + cyt c_y/cbb_3-C_{ox} + aa_3-C_{ox}	+	−	+	+	+	0.5	1.05	2.05	0.5

[a] Cyt *a*, cyt *b*, and cyt *c* values are expressed as nanomoles of heme per milligram of protein, using appropriate extinction coefficients, as described in Materials and Methods. Cyt *c* profiles are tabulated from the data in Fig. 4.

[b] ND, not detected.

Res growth of the cyt bc_1^- (BC17), cyt c_2^- cyt c_y^- (Gadc2cy), and cbb_3-C_{ox}^- aa_3-C_{ox}^- (ME127) mutants were consistent with the presence of an alternate respiratory pathway, involving a Q_{ox} (13). It was also noted that mutants lacking the cbb_3-C_{ox} (MT001, KD02, and especially KD04) formed highly pigmented colonies under respiratory growth conditions.

Next, the ability of all strains to perform the Nadi reaction (24), described in Materials and Methods, was tested as an indication of their C_{ox} activities. Among them, only the cbb_3-C_{ox}^- aa_3-C_{ox}^- mutant (ME127) exhibited a complete Nadi$^-$ phenotype (i.e., no blue color formation after more than 15 min of staining) (Table 2). The cbb_3-C_{ox}^- mutant (MT001) and its cyt c_2-cbb_3-C_{ox}^- (KD02) and cyt c_y^- cbb_3-C_{ox}^- (KD04) derivatives showed various degrees of Nadi^{slow} phenotypes (i.e., formation of a bluish color within a few minutes of staining), with KD04 being the most defective in this respect. The remaining mutants were Nadi$^+$ (i.e., formed a blue color in less than 1 min of staining), like the wild-type *R. sphaeroides* strain Ga. These observations indicated that absence of either the aa_3-C_{ox} (JS100), cyt c_2 (Gadc2), cyt c_y (Gadcy), or their combination (Gadc2cy, KD03, and KD05) did not affect the Nadi phenotype. Thus, in *R. sphaeroides*, the Nadi$^+$ phenotype correlated better with the presence of an active cbb_3-C_{ox} rather than an aa_3-C_{ox}. It was also noted that the Nadi phenotype of various mutants was affected by the presence or absence of the electron carriers cyt c_2 and cyt c_y and also by the growth conditions used. For example, the cyt c_y^- cbb_3-C_{ox}^- mutant KD04 exhibited a stronger Nadi$^+$ phenotype if younger colonies were stained, but conversely, the cyt c_2^- cbb_3-C_{ox}^- mutant KD02 became as Nadi$^-$ as the cbb_3-C_{ox}^- aa_3-C_{ox}^- mutant ME127 when grown in enriched YCC medium (30).

Cytochrome contents of various *R. sphaeroides* mutants. The contents of the *a*-, *b*-, and *c*-type cytochromes in chromatophore membranes, and in membrane supernatants, of various mutants grown by respiration in Med A were estimated using reduced-minus-oxidized optical absorption difference spectra (Fig. 3 and Table 2). Comparison of the reduced-minus-oxidized spectra of the cbb_3-C_{ox}^- (MT001) and cbb_3-C_{ox}^- aa_3-C_{ox}^- (ME127) mutants with other strains revealed significant decreases in the amounts of the *c*-, *b*-, and *a*-type cytochromes (peaks around 550, 560, and 605 nm, respectively) (Fig. 3A). In addition, contribution of the *b*- and *c*-type cyt subunits of the cyt bc_1 complex to total cytochrome contents of membranes was readily visible in the 550- to 560-nm region when the cyt bc_1^- mutant BC17 was compared to other mutants. Importantly, comparison of the cyt c_2^- cbb_3-C_{ox}^- (KD02), cyt c_y^- aa_3-C_{ox}^- (KD03), cyt c_y^- cbb_3-C_{ox}^- (KD04), and cyt c_2^- aa_3-C_{ox}^- (KD05) double mutants with their respective parents (cbb_3-C_{ox}^- [MT001] and aa_3-C_{ox}^- [JS100]) and with the wild-type strain Ga revealed that the 605-nm broad peak was absent in mutants carrying *ctaD*::*spe* and that the 550-nm peak was decreased significantly in those containing *ccoNO*::*kan*, as expected based on their genotypes (Fig. 3B).

In all mutants, the amount of *a*-type cytochromes was lower (e.g., as low as 0.24 ± 0.01 nmol/mg of protein in the cyt c_2^- cyt c_y^- mutant Gadc2cy) than in the wild-type strain Ga (0.8 ± 0.04 nmol/mg of protein) (Table 2). The *b*-type heme content was also low in almost all mutants (around 1.2 ± 0.3 nmol/mg of protein); an exception was the amount in the cyt c_y^- aa_3-C_{ox}^- (KD03) mutant, which was similar to that in Ga (2.2 ± 0.1 nmol/mg of protein). Further, the amounts of *c*-type cytochromes dropped from 3.8 ± 0.2 nmol/mg of protein in Ga to 0.7 ± 0.02 nmol/mg of protein in cyt c_2^- cbb_3-C_{ox}^- (KD02) and cyt c_y^- cbb_3-C_{ox}^- (KD04) mutants as a result of mutations eliminating various *c*-type cytochromes. Elimination of the cbb_3-C_{ox} decreased the total amount of the *b*-type cytochromes by about one-half and that of the *c*-type cytochromes by more than two-thirds. Consequently, the cyt *b*-to-cyt *c* ratios increased from 0.5 ± 0.04 in membranes of the cyt bc_1^- mutant (BC17) to 1.3 ± 0.1 in those of the cyt c_2^- cbb_3-C_{ox}^- mutant (KD02). Thus, clearly the contents of the *a*-, *b*-, and *c*-type cytochromes in membrane fragments from various strains varied as a function of the missing components.

The *c*-type cytochrome contents of chromatophore membrane supernatants of the mutants were also determined using ascorbate-reduced-minus-ferricyanide-oxidized optical difference spectra (not shown). The data indicated that *R. sphaeroides* mutants carrying a *cycA* knockout allele had about 1/10 of the 550-nm absorption peak found in a wild-type strain. The absorption maximum of the remaining ascorbate-reducible *c*-type cyt was shifted to 552 nm, consistent with it being isocyt c_2 (33). Moreover, supernatants of the cyt bc_1^- mutant BC17 contained about threefold more cyt c_2 than those of the wild-type strain Ga. The presence of increased amounts of cyt c_2 in supernatants of mutants lacking the cyt bc_1 complex has been observed previously in *R. capsulatus* (32).

Cyt *c* profile of mutants lacking components of the *c*-type cytochrome-dependent respiratory branch of *R. sphaeroides*. Chromatophore membrane proteins of the mutants were further analyzed using TMBZ–SDS-PAGE to determine the profiles of their *c*-type cytochromes. At least five major TMBZ-stained bands of molecular masses ranging from approximately 30 to 12 kDa were discernible in the wild-type strain Ga (Fig. 4). Under the separation conditions used here, the cyt c_p subunit of the cbb_3-C_{ox} and cyt c_1 subunit of the cyt bc_1 complex run together as an unresolved doublet, which was followed by the cyt c_o subunit of the cbb_3-C_{ox} and cyt c_y. Cyt c_2 ran ahead of the other *c*-type cytochromes, but not being membrane anchored, its amount varied in different samples. Additional *c*-type cytochromes of unidentified nature running behind cyt c_p were also visible, and one of them is likely to correspond to the dimethyl sulfoxide-inducible *dorC* product (25, 38). As expected, cyt c_y was absent in Gadcy, Gadc2cy, KD03, and KD04; similarly, Gadc2, Gadc2cy, KD02, and KD05 (Table 1) lacked cyt c_2 (18, 27). Equally, cyt c_o was missing in ME127 (cbb_3-C_{ox}^- aa_3-C_{ox}^-) and in MT001 (cbb_3-C_{ox}^-) and its derivatives. On the other hand, JS100 (aa_3-C_{ox}^-) was like the wild-type strain Ga with respect to its *c*-type cytochrome content. The overall spectral and TMBZ–SDS-PAGE data established that the cyt *c* profiles of various mutants were in agreement with their genotypes.

Respiratory electron flow and C_{ox} activities in various *R. sphaeroides* mutants. Using the above-described mutant, we probed first for the presence of the C_{ox} activity in chromatophore membranes of various mutants, using reduced horse heart cyt *c* as a substrate. As expected, in semiaerobically grown cells of all strains except the cbb_3-C_{ox}^- aa_3-C_{ox}^- mutant ME127, substantial amounts of C_{ox} activity were detected, although the cbb_3-C_{ox}^- mutants exhibited lower levels (data not shown). Next, a detailed characterization of the electron

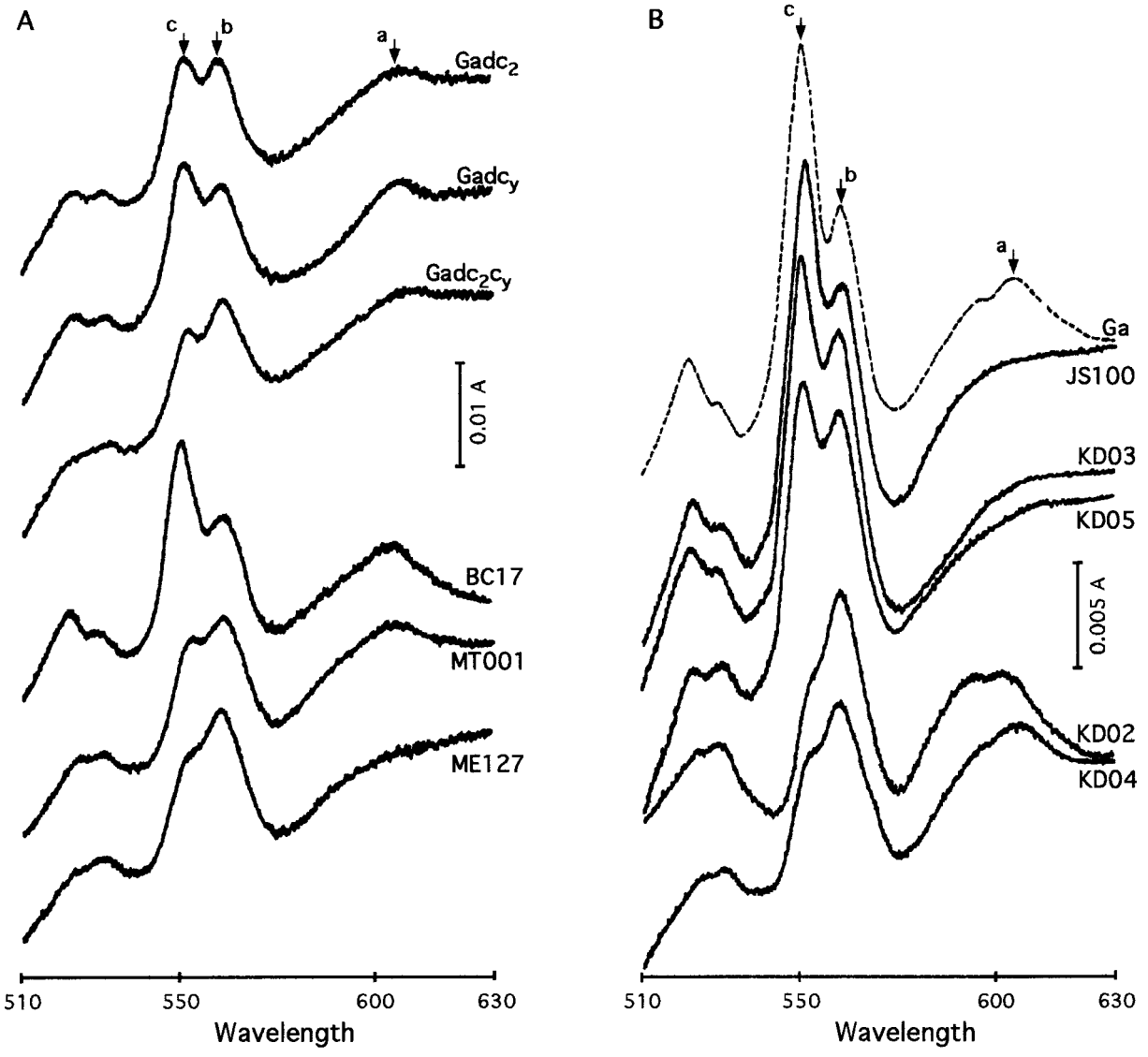

FIG. 3. Reduced-minus-oxidized optical absorption difference spectra of various *R. sphaeroides* mutants. The spectra were recorded between 510 and 630 nm at 25°C, using membrane fragments as described in Materials and Methods. (A) Spectra obtained with the cyt c_2^- (Gadc2), cyt c_y^- (Gadcy), cyt c_2^- cyt c_y^- (Gadc2cy), cyt bc_1^- (BC17), cbb_3-C_{ox}^- (MT001), and cbb_3-C_{ox}^- aa_3-C_{ox}^- (ME127) mutants; (B) those obtained with the wild-type strain Ga and the aa_3-C_{ox}^- (JS100), cyt c_y^-, aa_3-C_{ox}^- (KD03), cyt c_2^- aa_3-C_{ox}^- (KD05), cyt c_2^- cbb_3-C_{ox}^- (KD02), and cyt c_y^- cbb_3-C_{ox}^- (KD04) mutants. Absorption peaks corresponding to the *a*-, *b*-, and *c*-type cytochromes are indicated by arrows. Note that the absorbance scale used in panel A is twice as large as that in panel B.

flow through the different components of the respiratory chain was undertaken by using specific substrates and inhibitors. It is known that while addition of NADH or succinate activates electron transport via the respiratory dehydrogenases, inhibitors like antimycin A (Ant A) or Myx block it at the level of the cyt bc_1 complex (Fig. 1) (46). Respiratory capabilities of various mutants studied here were assessed directly by monitoring the rates of O_2 consumption depending on NADH or succinate, and in the presence or absence of exogenous cyt *c*, as performed previously with various *R. capsulatus* mutants (15).

Membrane fragments of the wild-type strain Ga rapidly oxidized various substrates, and the ensuing O_2 uptake was sensitive to Myx, dropping from 20.6 to 5.8 μmol of O_2 consumed/mg of protein/min in the presence of 2 μM of Myx (Table 3). Addition of 50 μM horse heart cyt *c* stimulated the rate of NADH oxidation to 30.9 μmol of O_2 consumed/mg of protein/min. This suggested that exogenous cyt *c* substituted well for the shortage of endogenous cyt c_2, which could have been depleted during cell disruption and membrane fragments preparation. Exogenous cyt *c* also greatly increased the rate of NADH oxidation (from 0.9 to 2.6 μmol of O_2 consumed/mg of protein/min) or ascorbate-C_{ox} activity (from 6.6 to 23.4 μmol of O_2 consumed/mg of protein/min) in the cyt c_2^- cyt c_y^- (Gadc2cy), cyt c_y^- aa_3-C_{ox}^- (KD03), and cyt c_y^- cbb_3-C_{ox}^- (KD04) mutants lacking the membrane-attached cyt c_y (Table 3). Moreover, pairwise comparison of various strains containing or lacking cyt c_y (i.e., Gadc2 versus Gadcy, KD02 versus KD04, and KD05 versus KD03) indicated that the presence of

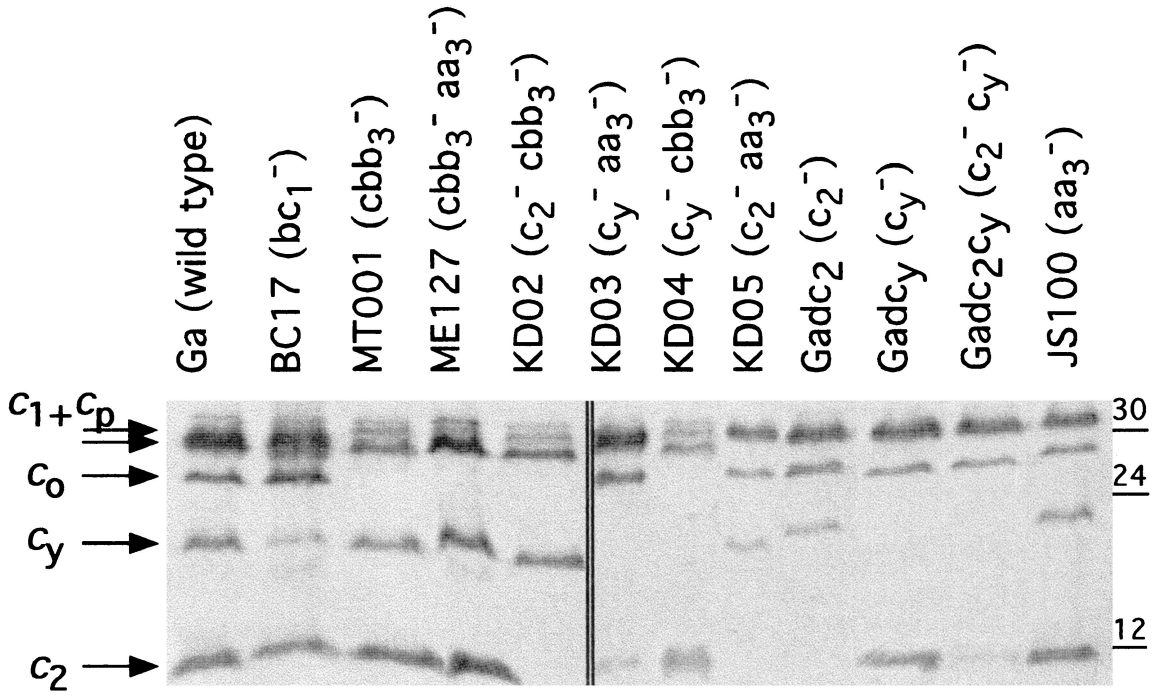

FIG. 4. *c*-type cytochromes detected in various *R. sphaeroides* mutants. Membrane fragments of various mutants were analyzed by SDS-PAGE, and *c*-type cytochromes were revealed via their peroxidase activities using TMBZ as described in Materials and Methods. c_1+c_p, c_o, c_y, and c_2 correspond to the cyt c_1 and c_p subunits of the cyt bc_1 complex and the cbb_3-C_{ox}, cyt c_o subunit of the cbb_3-C_{ox}, membrane-attached electron carrier cyt c_y, and soluble electron carrier cyt c_2, respectively. Additional unidentified *c*-type cytochromes running behind the doublet corresponding to cyt c_p+c_1 are also visible.

cyt c_y led almost in all cases to higher O_2 consumption activities. Thus, cyt c_y plays an important role as an electron carrier in the respiratory electron transport of *R. sphaeroides*, for in its absence the respiratory activities become more dependent on exogenous cyt *c*.

Remarkably, the artificial electron donor DCIP reduced cyt c_y better than cyt c_2, as indicated by the lower oxidative rates observed in its presence in appropriate mutants (e.g., cyt c_y^- cbb_3-C_{ox}^- [KD04] versus cyt c_2^- cbb_3-C_{ox}^- [KD02] mutants [3.6 versus 19.3 μmol of O_2 consumed/mg of protein/min], or cyt c_y^- aa_3-C_{ox}^- [KD03] versus cyt c_2^- aa_3-C_{ox}^- [KD05] mutants [23.0 versus 88.0 μmol of O_2 consumed/mg of protein/min]) (Table 3). The small amounts of C_{ox} activities detected in membranes of the cyt c_y^- cbb_3-C_{ox}^- (KD04) and cyt c_2^- cyt c_y^- (Gadc2cy) mutants using reduced DCIP (3.6 and 6.6 μmol of O_2 consumed/mg of protein/min, respectively) also differed from the increase of activity seen upon addition of cyt *c* (43.0 and 23.4 μmol of O_2 consumed/mg of protein/min, respectively). Thus, DCIP did not act as a good electron donor when cyt c_y and cbb_3-C_{ox} (KD04) or both cyt c_2 and cyt c_y (Gadc2cy) were absent, whereas horse heart cyt *c* acted as a good substitute for cyt c_2.

Interestingly, no more than one-fifth of the total O_2 consumption activity remained upon addition of either 2 μM Myx or 50 μM CN^- to membrane fragments of the wild-type strain Ga (Table 3). This remnant activity was in line with NADH oxidation detected in membranes of the cbb_3-C_{ox}^- aa_3-C_{ox}^- (ME127), cyt c_2^- cyt c_y^- (Gadc2cy), or cyt bc_1^- (BC17) mutant. Virtually no C_{ox} was detected in ME127 under all assay conditions, monitoring either NADH-, succinate-, or ascorbate-dependent O_2 consumption, and both in the presence and in the absence of exogenous cyt *c* (Table 3). The limited O_2 consumption activity detected was not inhibited by 0.1 mM CN^- and possibly corresponded to other some kind of terminal oxidase, such as Q_{ox} (13). On the other hand, the cyt bc_1^- mutant BC17 contained C_{ox} activities (39 or 42 μmol of 0.1 mM CN^--sensitive O_2 consumed/mg of protein/min when assayed with ascorbate plus DCIP or exogenous cyt *c*, respectively) comparable to those seen with the wild-type strain Ga

TABLE 3. Respiratory activities in membranes of various *R. sphaeroides* mutants grown by respiration[a]

Strain	Activity (μmol of O_2 consumed/mg of protein/min)							
	NADH				Succinate		Ascorbate	
	Alone	+Cyt *c*	+Myx	+Cyt *c*, +CN	Alone	+Cyt *c*	+DCIP	+Cyt *c*
Ga	20.6	30.9	5.8	6.2	6.9	8.3	56.0	57.0
KD02	5.2	7.7	2.2	2.3	4.7	7.5	19.3	34.0
KD04	2.3	4.9	1.1	1.2	2.0	6.0	3.6	43.0
KD03	4.8	12.0	4.1	4.4	4.8	8.8	23.0	88.0
KD05	15.3	19.2	5.0	5.2	4.8	8.0	88.0	92.0
JS100	9.6	11.7	0.6	0.5	4.8	7.5	44.0	35.0
MT001	8.9	11.1	1.2	1.1	5.2	8.8	26.0	33.0
Gadc2cy	0.9	2.6	1.0	0.9	0.9	2.6	6.6	23.4
Gadc2	7.7	7.9	1.2	1.3	2.7	3.4	22.7	33.6
Gadcy	2.0	3.6	1.4	1.3	2.3	3.7	25.4	22.2
ME127	5.3	6.3	5.1	5.3	4.6	5.6	1.3	2.6
BC17	3.8	3.8	3.7	3.7	3.8	3.8	39.0	41.8

[a] In these assays, 0.2 mM NADH, 5 mM succinate, 2 mM ascorbate, 0.2 mM DCIP, 50 μM horse heart cyt *c*, 50 μM CN^-, and 2 μM Myx were used as appropriate. Strain genotypes are given in Table 1.

(56 or 57 μmol of O_2/mg of protein/min using DCIP or cyt *c*, respectively). Lastly, the *cbb*$_3$-C_{ox}^- (MT001) and *aa*$_3$-C_{ox}^- (JS100) mutants contained about one-half of the total C_{ox} activity found in the wild-type strain Ga (11.7 and 11.1 μmol of O_2/mg of protein/min of NADH oxidase activity in the presence of exogenous cyt *c* in JS100 and MT001, respectively). Clearly, elimination of either the *cbb*$_3$-C_{ox} or the *aa*$_3$-C_{ox} decreased the total amount of the C_{ox} activity but did not abolish it completely (37).

Most striking findings were obtained using the cyt c_2^- *cbb*$_3$-C_{ox}^- (KD02), cyt c_y^- *aa*$_3$-C_{ox}^- (KD03), cyt c_y^- *cbb*$_3$-C_{ox}^- (KD04), and cyt c_2^- *aa*$_3$-C_{ox}^- (KD05) mutants, which contained simpler electron transport pathways beyond the cyt bc_1 complex (Fig. 1). The data indicated that higher O_2 consumption activities were found in mutants containing the *cbb*$_3$-C_{ox} (KD03 and KD05), and among them that harboring only cyt c_y (i.e., KD05) exhibited the highest C_{ox} activity. Conversely, lower O_2 consumption abilities were encountered in mutants lacking the *cbb*$_3$-C_{ox} (KD02 and KD04), and among them that lacking cyt c_y (i.e., KD04) exhibited the lowest activity (Table 3). Therefore, both cyt c_2 and cyt c_y donated electrons to both the *cbb*$_3$-C_{ox} and the *aa*$_3$-C_{ox} in vitro, but to different extents. The data suggested that the respiratory electron transfer pathways via the *cbb*$_3$-C_{ox} may be more active than those via the *aa*$_3$-C_{ox} subbranches in cells grown under semiaerobic conditions. However, the amounts of various components varied between various mutants (Table 2), precluding firmer conclusions. Further dissection of the C_{ox} activities into fractions corresponding to the *cbb*$_3$-C_{ox} and *aa*$_3$-C_{ox} activities exclusively linked to cyt c_2 or cyt c_y was impossible due to the assays used being unable to discriminate between the enzymes and their substrates.

NADH-induced cyt *c* oxidoreduction kinetics in various *R. sphaeroides* strains. NADH-induced cyt *c* oxidoreduction kinetics in membranes from wild-type and various *R. sphaeroides* mutants were monitored in the presence or absence of oxygen in order to assess directly the electron transfer abilities of cyt c_y and cyt c_2 to the *cbb*$_3$-C_{ox} and *aa*$_3$-C_{ox} enzymes. In the wild-type strain Ga, approximately 50% of the total *c*-type cytochromes in membranes were rapidly reduced (half-life [$t_{1/2}$] of <1 s) upon addition of NADH (Fig. 5). This respiration-dependent steady-state cyt *c* reduction (i.e., first reduction phase) lasted for several minutes, depending on the amount of membrane fragments used, and was sensitive to the cyt bc_1 complex inhibitors Myx and Ant A (2 μM each) (Fig. 5). Thus, a large fraction of the *c*-type cytochrome complement of membranes from wild-type cells is in rapid equilibrium with the respiratory electron transport system. Similar but slower oxidoreduction kinetics ($t_{1/2}$ = 1 to 2 s) were observed using membranes from the *aa*$_3$-C_{ox}^- (JS100), cyt c_2^- *aa*$_3$-C_{ox}^- (KD05), and cyt c_y^- *aa*$_3$-C_{ox}^- (KD03) mutants. Even slower cyt *c* reduction kinetics (2 s, $<t_{1/2}<$10 s) were seen with membranes from the *cbb*$_3$-C_{ox}^- (MT001), cyt c_2^- *cbb*$_3$-C_{ox}^- (KD02), and cyt c_y^- *cbb*$_3$-C_{ox}^- (KD04) mutants.

Upon depletion of O_2, and hence inhibition of the C_{ox} activities, cyt *c* reduction further increased in the wild-type strain Ga and in various *aa*$_3$-C_{ox}^- mutants to about 95% (second reduction phase). In the *cbb*$_3$-C_{ox}^- mutants, the amounts of the *c*-type cytochromes reduced under steady-state respiration were between 30 and 45% of their total content, reaching a maximum of about 50 to 60% under anaerobic conditions (Fig. 5). This second phase of cyt *c* reduction revealed the amount of cyt *c* that had been oxidized during the first phase when cyt *c* oxidases were active and hence illustrated at least partly electron conduction to these enzymes by their electron carriers. Therefore, the data obtained with mutants containing linear electron transport pathways between the cyt bc_1 complex and the cyt *c* oxidases demonstrated that both cyt c_2 and cyt c_y indeed donated electrons to either the *cbb*$_3$-C_{ox} or *aa*$_3$-C_{ox} enzyme. However, the cyt $c_y \rightarrow$ *aa*$_3$-C_{ox} (KD02) and cyt $c_2 \rightarrow$ *aa*$_3$-C_{ox} (KD04) pathways appeared to be less efficient (i.e., smaller second phases), suggesting that under our experimental conditions the *aa*$_3$-C_{ox} played in O_2 consumption a less prominent role than the *cbb*$_3$-C_{ox}.

The light-harvesting antenna complexes are induced in the presence of oxygen in *R. sphaeroides* mutants lacking either both cyt c_2 and cyt c_y or the *cbb*$_3$-C_{ox} activity (28, 29). During our studies we also noted that *R. sphaeroides* strain MT001 lacking the *cbb*$_3$-C_{ox} and its derivatives lacking in addition either cyt c_2 or cyt c_y (KD02 or KD04) formed highly pigmented colonies under Res growth conditions. This pigmentation was especially pronounced in a mutant lacking both cyt c_y and the *cbb*$_3$-C_{ox} (KD04). Indeed, spectral examination of chromatophore membranes of various mutants confirmed the presence of prominent absorption peaks in the 800- to 875-nm region (Fig. 6). Thus, the absence of the *cbb*$_3$-C_{ox} and its electron donors modulated the production of the light-harvesting complexes in the presence of oxygen. Remarkably, the pigment complexes were either absent or much less pronounced in the other *R. sphaeroides* Ga derivaties used in this work, including the *cbb*$_3$-C_{ox}^- *aa*$_3$-C_{ox}^- (ME127), cyt bc_1^- (BC17), and cyt c_2^- cyt c_y^- (Gadc2cy) mutants.

DISCUSSION

In this work we used a biochemical genetic approach, which consisted of disrupting simultaneously one of the two electron carrier *c*-type cytochromes and one of the two cyt *c* oxidases, to dissect the complicated respiratory electron transport pathways of *R. sphaeroides* (Fig. 1). The double mutants thus obtained simplified the crisscrossed pathways and enabled us to analyze the abilities of the different electron carriers to convey electrons from the cyt bc_1 complex to the terminal cyt *c* oxidases. Prior to this work, it was well known that the soluble cyt c_2 donates electrons to the *aa*$_3$-C_{ox}; indeed, it could be assumed correctly that it also donates electrons to the *cbb*$_3$-C_{ox} (15, 27). On the other hand, not much was known about the electron carrier properties of the more recently discovered membrane-anchored cyt c_y in *R. sphaeroides* (27, 51). Studies reported here confirmed for cyt c_2, and demonstrated for the first time for cyt c_y, that both are efficient electron donors to both the *cbb*$_3$-C_{ox} and the *aa*$_3$-C_{ox} during the respiratory growth of *R. sphaeroides*. Neither of the two electron carriers is restricted to function solely with either of the cyt *c* oxidases, and clearly all four subbranches appear to be functional (Fig. 1). Whether or not all of these pathways are also proficient in vivo to support respiratory growth of *R. sphaeroides* in the absence of its Q_{ox}-dependent alternate branch(es) remains to be seen.

At least under the semiaerobic growth conditions used here,

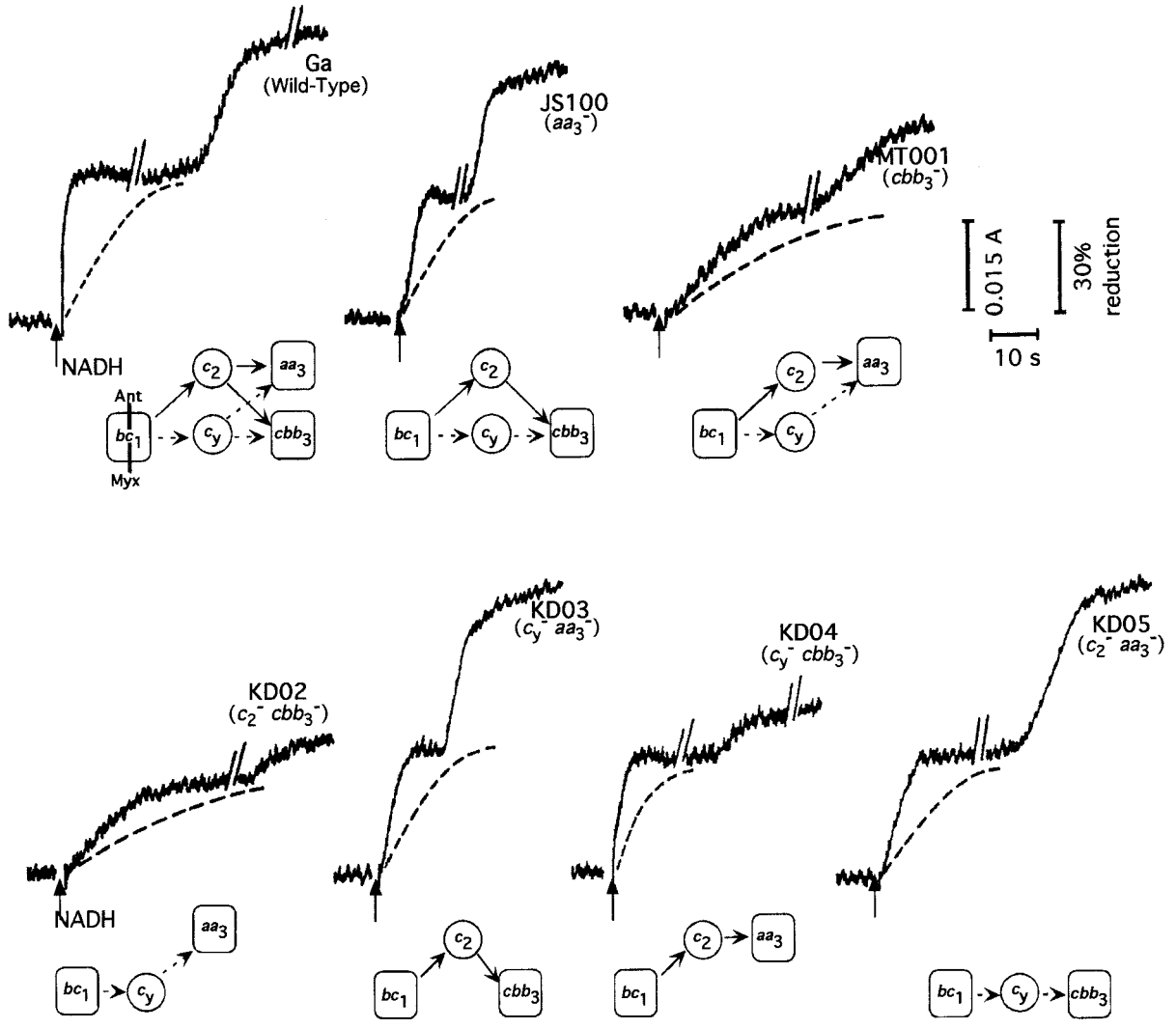

FIG. 5. Cyt *c* reduction kinetics in *R. sphaeroides* wild-type strain Ga and various mutants. Cyt *c* reduction kinetics were monitored at 551 to 540 nm using membrane fragments of various mutants as described in Materials and Methods. In all experiments, the first reduction wave was initiated by addition of 0.2 mM NADH at the time indicated by the arrow, while the second reduction wave followed the onset of anaerobiosis the time of which was dependent on the rate of oxygen consumption. Dashed traces represent cyt *c* reduction patterns observed upon addition of Ant A or Myx (2 μM each) before the addition of NADH. Protein concentrations of membrane fragments used were 0.8 mg/ml and 2 to 3 mg/ml for the wild-type strain Ga and its mutant derivatives, respectively. Below the traces, schemes depicting the available electron transport pathways are shown.

the cbb_3-C_{ox} subbranches appear to be more prominent in catalyzing electron transfer between the cyt bc_1 complex and the cyt *c* oxidases in vitro. However, whether this prominence is due to the larger amounts of the components of these pathways or to their better catalytic abilities remains unknown until determination of their amounts in each case. Among the electron carriers, while cyt c_2 can diffuse between the RC and the cyt bc_1 complexes of the photosynthetic electron transfer chains (10), cyt c_y is conceivably restricted to interact with a limited number of partners due to its membrane anchor (26, 27). Nonetheless, it is noteworthy that the alpha group proteobacterium *Rickettsia prowazekii*, thought to be closely related to mitochondria, lacks a soluble cyt *c* but contains a membrane-attached cyt c_y homologue (1, 23).

Availability of otherwise isogenic mutants lacking different *c*-type cytochromes of *R. sphaeroides* allowed us to identify each of these proteins unambiguously and confirmed our previous assignments of the cytochromes c_2, c_y, c_1, c_o, and c_p in *R. sphaeroides* (18, 27). It is noteworthy that in this bacterium cyt c_y runs ahead of the cyt c_o subunit of the cbb_3-C_{ox} (Fig. 3), which is different from what has been observed with *R. capsulatus* cyt c_y (26). Whether the inability of *R. sphaeroides* cyt c_y to donate electrons to the RC is linked to its smaller size remains to be seen (27).

The mutants described here, eliminating systematically various respiratory components, allowed us to estimate the amounts of various *b*- and *c*-type cytochromes present in membranes of *R. sphaeroides* cells grown under semiaerobic conditions. It appears that in a wild-type strain like Ga, elimination of the cbb_3-C_{ox} decreased roughly one-half of the total amount of the *b*-type cytochromes and two-thirds of the *c*-type cytochromes in membranes. Similarly, deletion of the cyt bc_1 com-

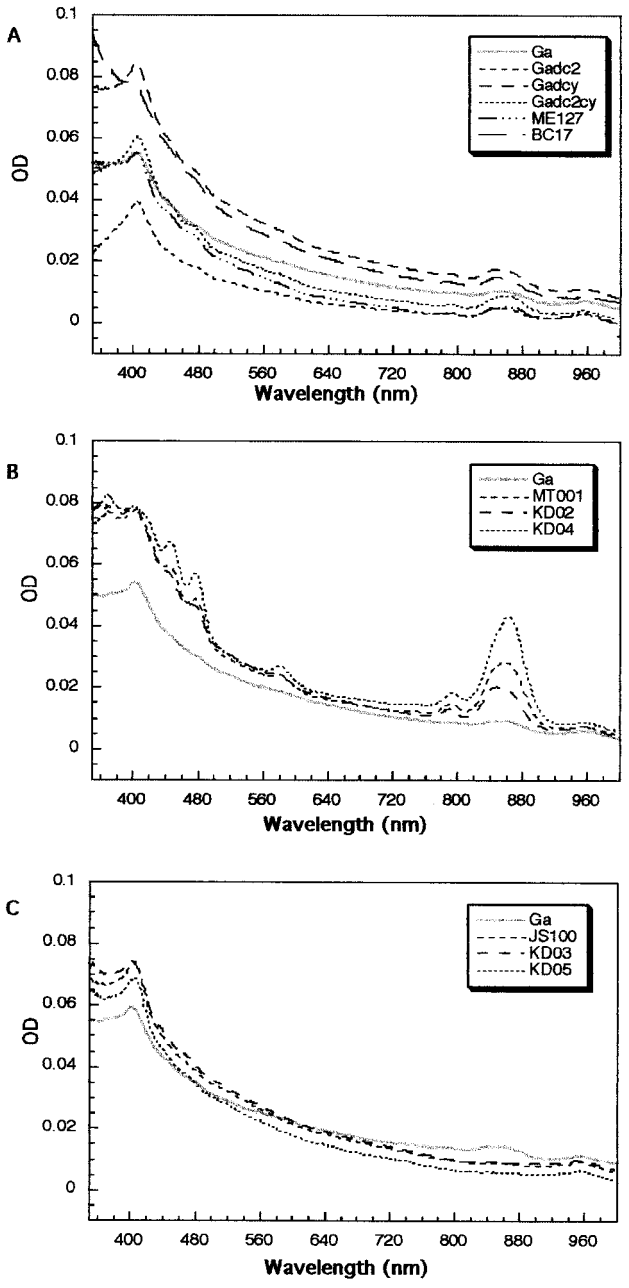

FIG. 6. Absorption spectra of membrane fragments of various *R. sphaeroides* mutants. Membrane fragments were prepared from cells grown by respiration at an optical density (OD) at 630 nm of 0.4, and their absorption spectra were recorded as described in Materials and Methods. Spectra were obtained for the wild-type strain Ga and the cyt c_2^- (Gadc2), cyt c_y^- (Gacy), cyt c_2^- cyt c_y^- (Gadc2cy), cbb_3-C_{ox}^- aa_3-C_{ox}^- (ME127), and cyt bc_1^- (BC17) mutants (A), the wild-type strain Ga and the cbb_3-C_{ox}^- (MT001), cyt c_2^- cbb_3-C_{ox}^- (KD02), and cyt c_y^- cbb_3-C_{ox}^- (KD04) mutants (B), and the wild-type strain Ga and the aa_3-C_{ox}^- (JS100), cyt c_y^- aa_3-C_{ox}^- (KD03), and cyt c_2^- aa_3-C_{ox}^- (KD05) mutants (C). See the text for further details.

plex also decreased about one-half of the total amount of both *b*- and *c*-type cytochromes. These estimations are in agreement with the subunit composition of the cbb_3-C_{ox} and the cyt bc_1 complex and suggest that these complexes may be present at similar amounts in *R. sphaeroides* membranes under the growth conditions used here. However, it should be noted that the amounts of various cytochromes change in different mutants as a function of the presence or absence of various components of the electron transport chain. For example, the absence of electron-carrying *c*-type cytochromes or the cyt bc_1 complex also decreased the amounts of the cbb_3-C_{ox} or the aa_3-C_{ox} (Table 3). Thus, caution should be exercised in extrapolating the results obtained using membrane fragments to intact cells grown under various physiological conditions.

Estimation of the C_{ox}-independent respiratory pathway in the wild-type strain Ga and in cbb_3-C_{ox}^- aa_3-C_{ox}^- (ME127), cyt bc_1^- (BC17), and cyt c_2^- cyt c_y^- (Gadc2cy) mutants indicated that in *R. sphaeroides* about one-fifth of the respiratory capacity is insensitive to 100 μM CN^- and is possibly mediated via a Q_{ox} enzyme(s). This situation is unlike that observed in *R. capsulatus* (15), where the analogous CN-resistant NADH-dependent respiration represents about 75 to 85% of NADH oxidation rate. Moreover, in *R. sphaeroides*, restraining the mitochondrial-like respiratory electron flow by eliminating some of its components does not affect the levels of CN-resistant respiration. Membranes of an *R. sphaeroides* mutant lacking the cyt c_2 and cyt c_y (Gadc2cy) exhibit very low NADH oxidation activity (Table 3), unlike its *R. capsulatus* counterpart FJ2 (cyt c_2^- cyt c_y^-), which has a CN-resistant NADH oxidation activity roughly three times higher than that of its parental wild-type strain MT1131 (15). This phenomenon was suggested to reflect a regulatory response of one of the respiratory branches over the other (49), but the molecular basis of this effect is unknown. No similar response is obvious in *R. sphaeroides*, for the mutants analyzed here exhibited a CN-resistant respiratory activity similar to that present in the wild-type membranes. The marked inefficiency of the alternate respiratory pathway, in addition to the photosynthetic incompetence of cyt c_y and the presence of an aa_3-C_{ox}, constitutes yet another striking difference between the growth abilities of the closely related species *R. capsulatus* and *R. sphaeroides*.

Increased synthesis of the photosynthetic apparatus in the presence of oxygen in mutants lacking the cbb_3-C_{ox} has been documented previously in *R. sphaeroides* strain 2.4.1 (28, 52). Recently, a similar situation has also been described in derivatives of the same strain lacking either the cyt bc_1 complex or the cytochromes c_2 and c_y (29). In these mutants, expression of the photosynthetic apparatus is not repressed by O_2, unlike in the wild-type strain, thus leading to the accumulation of increased amounts of light-harvesting antenna complexes and photosynthetic pigments. In *R. sphaeroides* strain Ga and its derivatives used here, the light-harvesting complexes were also highly induced in the cbb_3-C_{ox}^- (MT001), cyt c_2^- cbb_3-C_{ox}^- (KD02), and especially cyt c_y^- cbb_3-C_{ox}^- (KD04) mutants, while this induction was less apparent in the cyt bc_1^- (BC17), cbb_3-C_{ox}^- aa_3-C_{ox}^- (ME127), and cyt c_2^-, cyt c_y^- (Gadc2cy) mutants. Why similar mutants derived from *R. sphaeroides* strains 2.4.1 and Ga behave differently in this respect is unclear. In any event, close examination of the electron transport pathways (Fig. 1) suggests that either restricting the electron flow via the cbb_3-C_{ox} subbranches, as proposed earlier (29, 52), or forcing this flow via the aa_3-C_{ox} subbranches, or even a combination of these possibilities, may lead to the accumulation of the pigment proteins. Clearly, the creation of an imbalance between the aa_3-C_{ox} and cbb_3-C_{ox} subbranches with-

out taking into account the availability of O_2 might explain at least partly the pigmentation phenotypes observed in various mutants used in this work.

In summary, the work presented here establishes for the first time that both of the electron carriers cyt c_2 and cyt c_y are efficient electron donors to both the cbb_3-C_{ox} and the aa_3-C_{ox} during the respiratory growth of *R. sphaeroides*. It remains to be seen whether or not the electron flow via each of the subbranches defined here is alone sufficient to support the Res growth of *R. sphaeroides* under physiological growth conditions.

ACKNOWLEDGMENTS

This work was supported by DOE grants 91ER20052 to F.D., CRP/TUR99-01 to S.M., and MURST-COFIN 99 to D.Z.

We thank E. Darrouzet for help with the figures and critical reading of the manuscript.

REFERENCES

1. **Andersson, S. G., A. Zomorodipour, J. O. Andersson, T. Sicheritz-Ponten, U. C. M. Alsmark, R. M. Podowski, A. K. Naslund, A.-S. Ericksonn, H. H. Winkler, and C. G. Kurland.** 1998. The genome sequence of *Rickettsia prowazekii* and the origin of mitochondria. Nature **396:**133–140.
2. **Bradford, M. M.** 1976. A rapid and sensitive method for quantitation of microgram quantities of protein utilizing the principle of protein-dye binding. Anal. Biochem. **72:**248–254.
3. **Caffrey, M., E. Davidson, M. Cusanovich, and F. Daldal.** 1992. Cytochrome c_2 mutants of *Rhodobacter capsulatus*. Arch. Biochem. Biophys. **292:**419–426.
4. **Choudhary, M., C. Mackenzie, N. J. Mouncey, and S. Kaplan.** 1999. RsGDB, the *Rhodobacter sphaeroides* genome database. Nucleic Acids Res. **27:**61–62.
5. **Clayton, R. K.** 1963. Spectroscopic analyses of bacteriochlorophylls *in vitro* and *in vivo*. Photochem. Photobiol. **5:**669–677.
6. **Daldal, F., E. Davidson, and S. Cheng.** 1987. Isolation of the structural genes for the Rieske Fe-S protein, cytochrome *b* and cytochrome c_1, all components of the ubiquinol: cytochrome *c* oxidoreductase complex of *Rhodopseudomonas capsulata*. J. Mol. Biol. **195:**1–12.
7. **Daldal, F., S. Cheng, J. Applebaum, E. Davidson, and R. C. Prince.** 1986. Cytochrome c_2 is not essential for photosynthetic growth of *Rhodopseudomonas capsulata*. Proc. Natl. Acad. Sci. USA **83:**2012–2016.
8. **Donohue, T. J., A. G. McEwan, S. Van Doren, A. R. Crofts, and S. Kaplan.** 1988. Phenotypic and genetic characterization of cytochrome c_2 deficient mutants of *Rhodobacter sphaeroides*. Biochemistry **27:**1918–1925.
9. **Fellay, R., J. Frey, and H. Krisch.** 1987. Interposon mutagenesis of soil and water bacteria: a family of DNA fragments designed for in vitro insertional mutagenesis of Gram-negative bacteria. Gene **52:**147–153.
10. **Fernandez-Valesco, J., and A. R. Crofts.** 1991. Complexes or supercomplexes: inhibitor titrations show that electron transfer in chromatophores from *Rhodobacter sphaeroides* involves a dimeric UQH2:cyt c_2 oxidoreductase, and is delocalized. Biochem. Soc. Trans. **19:**588–593.
11. **Fonstein, M., T. Nikolskaya, Y. Kogan, and R. Haselkorn.** 1998. Genome encyclopedias and their use for comparative analysis of *Rhodobacter capsulatus* strains. Electrophoresis **19:**469–477.
12. **Garcia-Horsman, J. A., E. Berry, J. P. Shapleigh, J. O. Alben, and R. B. Gennis.** 1994. A novel cytochrome *c* oxidase from *Rhodobacter sphaeroides* that lacks Cu_A. Biochemistry **33:**3113–3119.
13. **Garcia-Horsman, J. A., B. Barquera, J. Rumbley, J. Ma, and R. B. Gennis.** 1994. The superfamily of heme-copper respiratory oxidases. J. Bacteriol. **176:**5587–6000.
14. **Gray, K. A., M. Grooms, H. Myllykallio, C. Moomaw, C. Slaughter, and F. Daldal.** 1994. *Rhodobacter capsulatus* contains a novel *cb*-type cytochrome *c* oxidase without a Cu_A center. Biochemistry **33:**3120–3127.
15. **Hochkoeppler, A., F. E. Jenney, Jr., S. E. Lang, D. Zannoni, and F. Daldal.** 1995. Membrane-associated cytochrome c_y of *Rhodobacter capsulatus* is an electron carrier from the cytochrome bc_1 complex to the cytochrome *c* oxidase during respiration. J. Bacteriol. **177:**608–613.
16. **Hosler, J. P., J. Fetter, M. M. Tecklenburg, M. Espe, C. Lerma, and S. Ferguson-Miller.** 1992. Cytochrome aa_3 of *Rhodobacter sphaeroides* as a model for mitochondrial cytochrome *c* oxidase. Purification, kinetics, proton pumping and spectral properties. J. Biol. Chem. **267:**24264–24272.
17. **Jenney, F. E., and F. Daldal.** 1993. A novel membrane-associated *c*-type cytochrome, cyt c_y can mediate the photosynthetic growth of *Rhodobacter capsulatus* and *Rhodobacter sphaeroides*. EMBO J. **12:**1283–1292.
18. **Jenney, F. E., R. C. Prince, and F. Daldal.** 1996. The membrane-bound cytochrome c_y of *Rhodobacter capsulatus* is an electron donor to the photosynthetic reaction of *Rhodobacter sphaeroides*. Biochim. Biophys Acta **1273:**159–164.
19. **Koch, H.-G., O. Hwang, and F. Daldal.** 1998. Isolation and characterization of *Rhodobacter capsulatus* mutants affected in cytochrome cbb_3 oxidase activity. J. Bacteriol. **180:**969–978.
20. **Koch, H.-G., C. Winterstein, A. S. Saribas, J. O. Alben, and F. Daldal.** 2000. Roles of the *ccoGHIS* gene products in the biogenesis of the cbb_3-type cytochrome *c* oxidase. J. Mol. Biol. **297:**49–65.
21. **La Monica, R. F., and B. L. Marrs.** 1976. The branched respiratory system of photosynthetically grown *Rhodopseudomonas capsulata*. Biochim. Biophys. Acta **423:**431–439.
22. **Lowry, O. H., N. J. Rosebrough, A. L. Farr, and R. J. Randall.** 1951. Protein measurement with the Folin phenol reagent. J. Biol. Chem. **193:**265–275.
23. **Margulis, L.** 1981. Symbiosis in cell evolution. W. H. Freeman, New York, N.Y.
24. **Marrs, B. L., and H. Gest.** 1973. Genetic mutations affecting the respiratory electron transport system of the photosynthetic bacterium *Rhodopseudomonas capsulata*. J. Bacteriol. **114:**1045–1051.
25. **Mouncey N. J., M. Choudhary, and S. Kaplan.** 1997. Characterization of genes encoding dimethyl sulfoxide reductase of *Rhodobacter sphaeroides* 2.4.1T: an essential metabolic gene function encoded on chromosome II. J. Bacteriol. **179:**7617–7624.
26. **Myllykallio, H., F. E. Jenney, Jr., C. Slaughter, and F. Daldal.** 1997. Cytochrome c_y of *Rhodobacter capsulatus* is attached to the cytoplasmic membrane by an uncleaved signal sequence-like anchor. J. Bacteriol. **179:**2623–2631.
27. **Myllykallio, H., D. Zannoni, and F. Daldal.** 1999. *Rhodobacter sphaeroides* cyt c_y is a membrane-attached electron carrier that is deficient in photosynthesis but proficient in respiration. Proc. Natl. Acad. Sci. USA **96:**4348–4353.
28. **Oh, J.-I., and S. Kaplan.** 1999. The cbb_3 terminal oxidase of *Rhodobacter sphaeroides* 2.4.1: structural and functional implications for the regulation of spectral complex formation. Biochemistry **38:**2688–2696.
29. **Oh, J.-I., and S. Kaplan.** 2000. Redox signaling: globalization of gene expression. EMBO J. **19:**4237–4247.
30. **Paddock, M. L., S. H. Rongey, G. Feher, and M. Y. Okamura.** 1989. Pathway of proton transfer in bacterial reaction centers: replacement of glutamic acid 212 in the L subunit by glutamine inhibits quinone (secondary acceptor) turnover. Proc. Natl. Acad. Sci. USA **86:**6602–6606.
31. **Prentki, P., and H. M. Krisch.** 1984. *In vitro* insertional mutagenesis with a selectable DNA fragment. Gene **29:**303–313.
32. **Prince, R. C., and F. Daldal.** 1987. Physiological electron donors to the photochemical reaction center of *Rhodobacter capsulatus*. Biochim. Biophys. Acta **894:**370–378.
33. **Rott, M. A., V. C. Witthuhn, B. A. Schilke, M. Soranno, A. Ali, and T. J. Donohue.** 1993. Genetic evidence for the role of isocytochrome c_2 in photosynthetic growth of *Rhodobacter sphaeroides spd* mutants. J. Bacteriol. **175:**358–366.
34. **Sasaki, T., Y. Notokawa, and G. Kikuchi.** 1970. Occurrence of both *a*-type and *o*-type cytochromes as the functional terminal oxidases in *Rhodopseudomonas sphaeroides*. Biochim. Biophys. Acta **197:**284–291.
35. **Schägger, H., and G. von Jagow.** 1987. Tricine-sodium dodecyl sulfate polyacrylamide gel electrophoresis for the separation of proteins in the range from 1 to 100 kDa. Anal. Biochem. **166:**368–379.
36. **Shapleigh, J. P., and R. B. Gennis.** 1992. Cloning, sequencing and deletion from the chromosome of the gene encoding subunit I of the aa_3-type cytochrome *c* oxidase of *Rhodobacter sphaeroides*. Mol. Microbiol. **6:**635–642.
37. **Shapleigh, J. P., J. J. Hill, J. O. Alben, and R. B. Gennis.** 1992. Spectroscopic and genetic evidence for two heme-Cu-containing oxidases in *Rhodobacter sphaeroides*. J. Bacteriol. **174:**2338–2343.
38. **Shaw, A., A. Hochkoeppler, P. Bonora, D. Zannoni, G. Hanson, and A. McEwan.** 1999. Characterization of DorC from *Rhodobacter capsulatus*, a *c*-type cytochrome involved in electron transfer to dimethyl sulfoxide reductase. J. Biol. Chem. **274:**9911–9914.
39. **Simon, R., U. Priefer, and A. Puhler.** 1983. A broad host range mobilization system for *in vivo* genetic engineering: transposon mutagenesis in Gram negative bacteria. Bio/Technology **1:**784–791.
40. **Sistrom, W.** 1960. A requirement for sodium in the growth of *Rhodopseudomonas sphaeroides*. J. Gen. Microbiol. **22:**778–785.
41. **Thomas, P. E., D. Ryan, and D. W. Levin.** 1976. An improved staining procedure for the detection of the peroxidase activity of cytochrome *P*-450 on sodium dodecyl sulfate polyacrylamide gels. Anal. Biochem. **75:**168–176.
42. **Toledo-Cuevas, M., B. Barquera, R. B. Gennis, M. Wikstrom, and J. A. Garcia-Horsman.** 1998. The cbb_3-type cytochrome *c* oxidase from *Rhodobacter sphaeroides*, a proton-pumping heme-copper oxidase. Biochim. Biophys. Acta **1365:**421–434.
43. **Williams, J., L. Steiner, and G. Feher.** 1986. Primary structure of the reaction center from *Rhodopseudomonas sphaeroides*. Proteins **11:**312–325.
44. **Youvan, D., E. Bylina, M. Alberti, H. Begusch, and J. Hearst.** 1984. Nucleotide and deduced polypeptide sequences of the photosynthetic reaction-center, B870 antenna, and flanking polypeptides from *Rhodopseudomonas capsulata*. Cell **37:**949–957.
45. **Yun, C.-H., R. Beci, A. R. Crofts, S. Kaplan, and R. B. Gennis.** 1990. Cloning and DNA sequencing of the *fbc* operon encoding the cytochrome bc_1 complex from *Rhodobacter sphaeroides*. Eur. J. Biochem. **194:**399–411.

46. **Zannoni, D.** 1995. Aerobic and anaerobic electron transport chains in anoxygenic phototrophic bacteria, p. 949–971. *In* R. E. Blankenship, M. T. Madigan, and C. E. Bauer (ed.), Anoxygenic photosynthetic bacteria. Kluwer Academic Publishers, Dordrecht, The Netherlands.
47. **Zannoni, D., and F. Daldal.** 1993. The role of *c*-type cytochromes in catalyzing oxidative and photosynthetic electron transport in the dual functional plasmamembrane of facultative phototorophs. Arch. Microbiol. **160:**413–423.
48. **Zannoni, D., B. A. Melandri, and A. Baccarini-Melandri.** 1976. Composition and function of the branched oxidase system in wild type and respiratory mutants of *Rhodopseudomonas capsulata*. Biochim. Biophys. Acta **423:**413–430.
49. **Zannoni, D., and A. L. Moore.** 1990. Measurement of the redox state of the ubiquinone pool in *Rhodobacter capsulatus* membrane fragments. FEBS Lett. **271:**123–127.
50. **Zannoni, D., G. Venturoli, and F. Daldal.** 1992. The role of the membrane bound cytochromes of *b*- and *c*-type in the electron transport chain of *Rhodobacter capsulatus*. Arch. Microbiol. **157:**367–374.
51. **Zeilstra-Ryalls, J., and S. Kaplan.** 1995. Aerobic and anaerobic regulation in *Rhodobacter sphaeroides* 2.4.1: role of the *fnrL* gene. J. Bacteriol. **177:**6422–6431.
52. **Zeilstra-Ryalls, J., M. Gomelsky, J. M. Eraso, A. Yeliseev, J. O'Gara, and S. Kaplan.** 1998. Control of photosystem formation in *Rhodobacter sphaeroides*. J. Bacteriol. **180:**2801–2809.